ОБЪЕДИНЕННЫЙ
ИНСТИТУТ
ЯДЕРНЫХ
ИССЛЕДОВАНИЙ
ДУБНА

E7 - 9974

A.G.Artukh, G.F.Gridnev, V.L.Mikheev, V.V.Volkov

SOME REGULARITIES IN THE PRODUCTION OF ISOTOPES WITH $4 \leq Z \leq 9$ IN THE INTERACTION OF ^{22}Ne WITH ^{232}Th

1976

E7 - 9974

A.G.Artukh, G.F.Gridnev, V.L.Mikheev, V.V.Volkov

SOME REGULARITIES IN THE PRODUCTION OF ISOTOPES WITH $4 \leq Z \leq 9$ IN THE INTERACTION OF ^{22}Ne WITH ^{232}Th

Submitted to "Nuclear Physics"

S u m m a r y

In the bombardment of ^{232}Th with ^{22}Ne ions with an energy of 172 MeV the energy spectra and production cross sections for isotopes of elements ranging from Be to F have been measured at an emission angle of 12°. It is shown that all the isotopes detected have been produced by deep inelastic collisions of the initial nuclei, i.e., the kinetic energies of the reaction products are close to the exit Coulomb barriers. It is found that the energy spectra widths (FWHM), relative yields at 12° and 40° and the Q_{gg}-dependences of isotopic production cross sections differ considerably for stable, neutron-deficient and neutron-rich isotopes. This difference can be interpreted as being due to a contribution from secondary processes such as α-particle and nucleon evaporation from the excited ^{22}Ne and light transfer reaction products. The data obtained can be employed to choose optimal conditions for the detection of the extremely neutron-rich isotopes of light elements produced in multinucleon transfer reactions.

1. Introduction

The studies of the interaction between complex nuclei have led to the discovery of the new type of heavy ion reactions termed as deep inelastic transfers (DIT)or quasi-fission (QF)[1-8]. A distinctive feature of the new reaction is that it combines the properties of both direct processes and compound nucleus decay. Like direct reactions, the DIT keeps a strong coupling between the entrance and exit channles. The angular distributions of DIT products are asymmetric. Light reaction products are emitted mostly in the forward direction. The mass and charge distributions of DIT products are crowded around A and Z of the initial nuclei. At the same time, the kinetic energy of the products is close to the exit Coulomb barrier and is practically independent of the initial collision energy. The latter feature of the DIT reminds us of the decay of a compound nucleus.

Transfer reactions occurring in the bombardment of ^{232}Th with 172 MeV ^{22}Ne ions have been investigated by us previously (ref.[5]).Using a $\Delta E, E$ telescope we

detected light products with $4 \leq Z \leq 9$ without isotope separation. It was shown that with a decrease in the emission angle a contribution from quasi-elastic transfers to the element production cross section decreases, and at angles of about 20° and less all transfer reactions belong to deep inelastic processes. In the present paper an attempt has been made to study in more detail different reaction channels of the DIT for the same system, $^{232}Th + ^{22}Ne$, at a bombarding energy of 172 MeV. The measurements were carried out at a lab.angle of 12°. The energy spectra and differential cross sections for the production of Be – F isotopes were measured. The data obtained are compared with those for an angle of 40°, which is close to the grazing angle of 51°. The contribution from secondary processes to the production cross sections for different isotopes is discussed. The data obtained are considered also from the viewpoint of producing the extremely neutron-rich isotopes of light elements.

2. Experimental Technique

The experiments have been performed using an external beam from the U-300 heavy ion cyclotron of the JINR Laboratory of Nuclear Reactions. The ^{22}Ne ion energy was equal to 174 MeV, and the average particle flux was about 10^{12} particles/sec. A metallic thorium target, 2.5 mg/cm^2 thick, was placed in the entrance focus of a magnetic spectrometer. Light transfer reaction products emitted at an angle of 12° with respect

to the beam direction in a solid angle of 3×10^{-3} sr were detected. The identification of reaction products by A and Z was carried out using the magnetic analysis combined with the ΔE, E technique [9]. The telescope of a thin semiconductor detector, ΔE, and a full absorption detector E was placed in the focal plane of the magnetic analyzer. The thickness and diameter of the ΔE detector were 27μm and 16 mm, respectively. Under these conditions the energy resolution of the spectrometer was about 2.5%. The energy spectra of the DIT products have the form of smooth curves with one maximum each. Since their widths reach several tens of MeV the energy resolution mentioned was sufficient. After being amplified, signals from the ΔE and E detectors were sent to a pulse-height analyzer operated in a two-dimensional mode, $128(\Delta E) \times 64(E)$. The beam was monitored by elastically scattered ions detected by a semiconductor detector placed at an angle of 30° with respect to the beam direction.

The energy spectra were obtained by measuring the yields of reaction products at different values of the spectrometer magnetic field. The magnetic field was measured by the nuclear resonance method. The yields of each isotope in different charge states were summed up. The absolute cross section values were determined by normalizing the isotopic yields to the yield of elastically scattered ions.

3. Experimental Results

3.1. Energy Spectra

The energy spectra of the isotopes of elements with $4 \leq Z \leq 9$ in the c.m. system are presented in figs. 1 and 2. The ^{22}Ne ion energy of 172 MeV indicated corresponds to the target half-thickness. In transforming the experimental data from the lab. system to the c.m. system the isotopes were assumed to be produced in two-body reactions. The reaction Q values are also shown in figs.1 and 2. The $\bar{Q}$ quantity is an average Q value for the isotopes of a given element. The Q variations with mass number A as one goes from neutron-rich to neutron-deficient isotopes of the given element do not exceed 3 MeV. Arrows show the energies gained by light reaction products in the exit channel at the expense of Coulomb forces. The exit Coulomb barriers are calculated for touching spherical nuclei with the nuclear parameter $r_o = 1.46$ fm /10/.

In figs.1 and 2 one can see that the isotopic yield maxima correspond to energies slightly above the Coulomb barriers. The difference between the energy in the maximum and the exit Coulomb barrier somewhat increases with increasing isotopic mass number (for a given element). The width of the energy spectra increases with Z . One can also notice the tendency of the energy spectra to become narrow as one goes from stable and neutron-deficient isotopes to neutron-rich ones. These characteristics of the energy spectra as a function of A and Z of the isotopes are shown explicitly in figs.3 and 4.

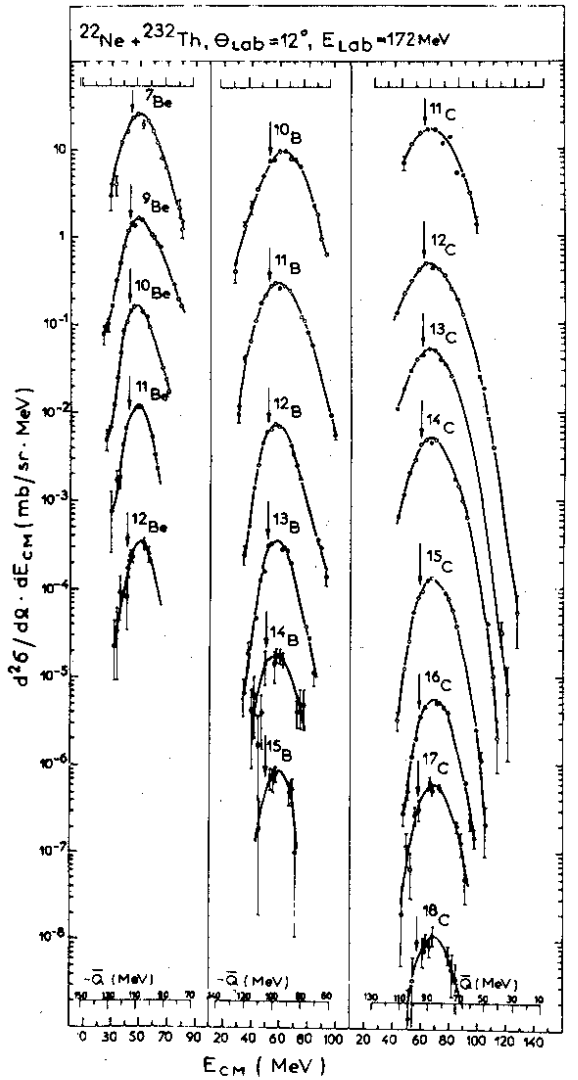

Fig.1. The c.m. energy spectra of Be, B and C isotopes produced by bombarding ^{232}Th with 172 MeV ^{22}Ne ions. Detection angle is 12°. Arrows show the exit Coulomb barriers calculated for touching spherical nuclei with r_o = 1.46 fm. $\bar{Q}$ is the average Q value. Experimental points are multiplied by factors as follows: ^{7}Be, ^{11}C(x1.5x10^{3}); ^{10}B(x1.5x10^{2}); ^{9}Be (x1.5x10^{1}); ^{10}Be, ^{11}Be, ^{11}B, ^{12}C(x.1.5); ^{12}Be, ^{12}B, ^{13}C(x1.5x10^{-1}); ^{13}B, ^{14}B, ^{14}C(x1.5x10^{-2}); ^{15}B, ^{15}C(x1.5x10^{-3}); ^{16}C, ^{17}C(x1.5x10^{-4}); ^{18}C(x1.5x10^{-5}).

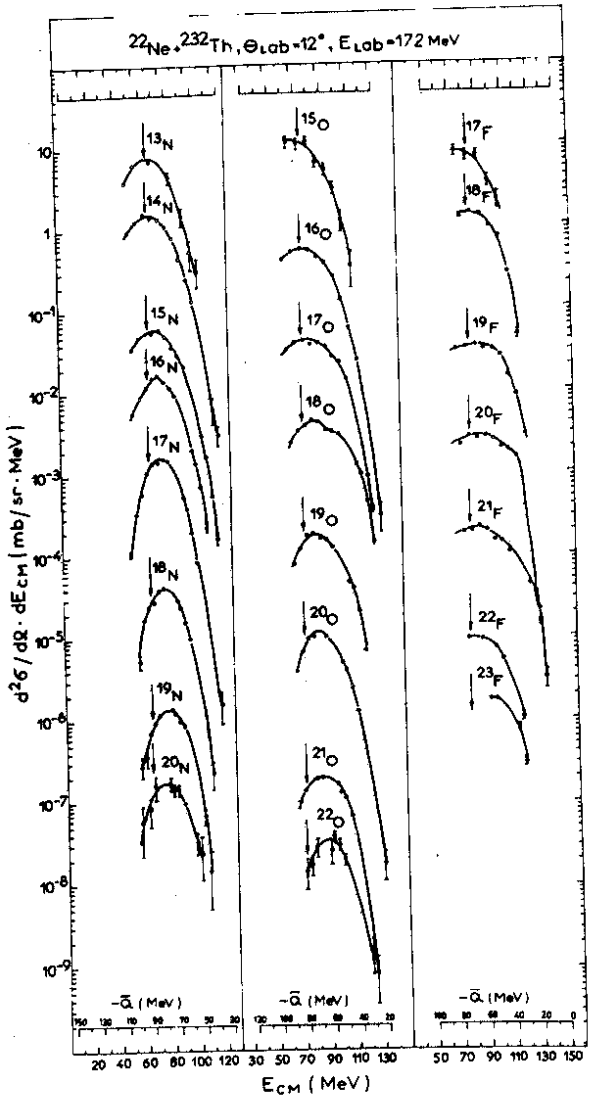

Fig.2. The same as in fig.1, for N, O and F isotopes with the following multiplication factors: ^{13}N, ^{15}O, ^{17}F(x1.5x10^{3}); ^{14}N, ^{18}F(x1.5x10^{1}); ^{16}O(x1.5); ^{15}N, ^{16}N, ^{17}O, ^{19}F(x1.5x10^{-1}); ^{17}N, ^{18}O, ^{20}F(x1.5x10^{-2}); ^{18}N, ^{19}O, ^{21}F(x1.5x10^{-3}); ^{19}N, ^{20}N, ^{20}O, ^{22}F, ^{23}F(x1.5x10^{-4}); ^{21}O, ^{22}O(x1.5x10^{-5}).

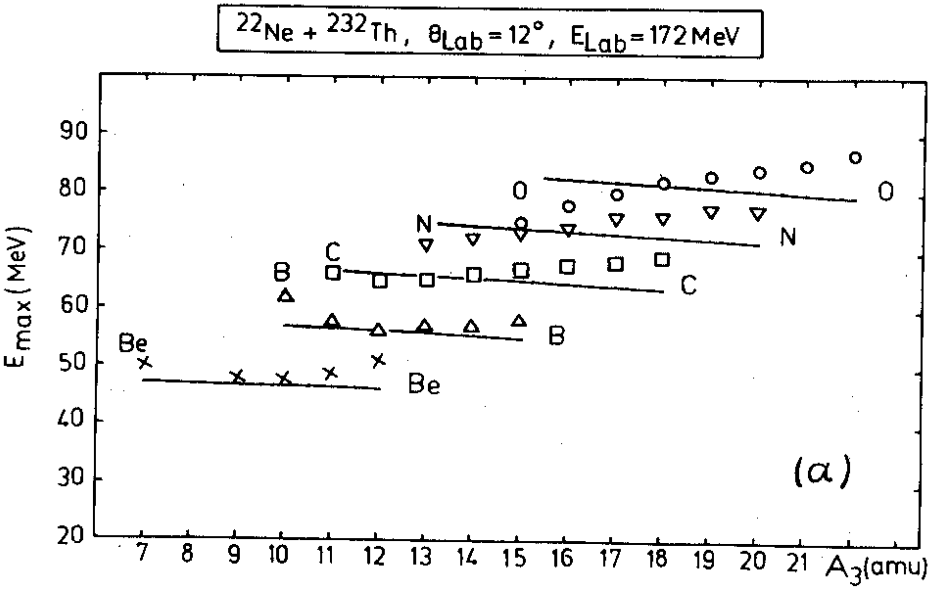

Fig.3a. The energy in the maximum of energy spectra E_{max} as a function of mass number A. The solid line shows the sums of the Coulomb and centrifugal barriers in the exit channel, $E_c + E_\ell$. The data are in the CMS.

In fig.3a, the energies E_{max} corresponding to the maximum isotopic yields are compared with the sum of the exit Coulomb and centrifugal barriers, E_c and E_ℓ, (solid line). In Fig.3b, the same comparison is made for $\overline{E}_{max}$, the average value of E_{max} for the isotopes of a given element. The dashed and solid lines show the calculated values for E_c and $(E_c + E_\ell)$, respectively. The data for E_{max} obtained by

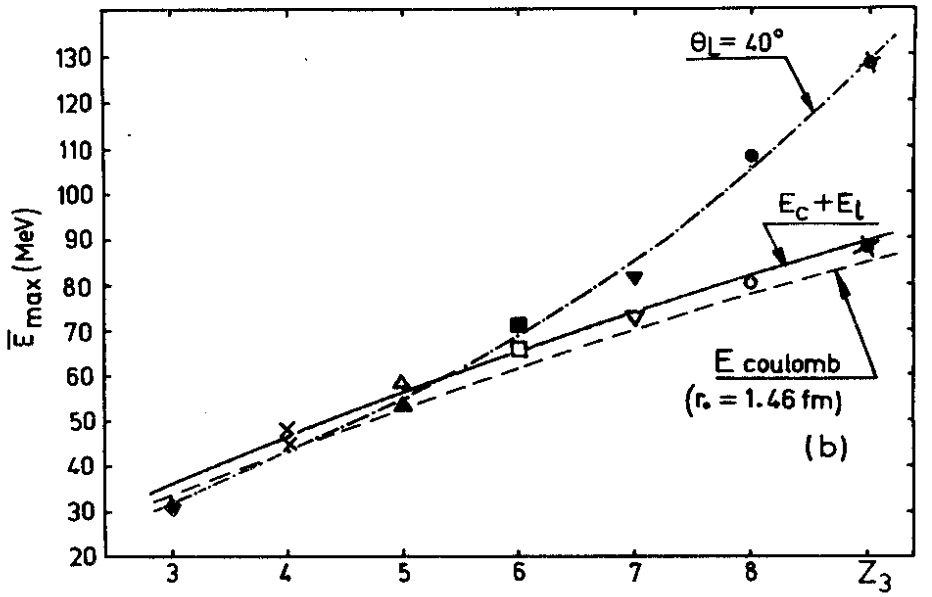

Fig.3b. The average values of E_{max} for the isotopes of a given element. Closed and open circles show the experimental values of E_{max} for 40° and 12°, respectively. The dashed line shows the calculated average value of E_c for the same isotopes at $r_o = 1.46$ fm. The solid line shows the calculated values of $E_c + E_\ell$.

bombarding ^{232}Th with 172 MeV ^{22}Ne ions at a detection angle of 40° (ref.[11]) are also presented in fig.3b. They are shown by closed marks and a dash-dotted curve drawn through them. In our calculations of the exit centrifugal barriers E_ℓ we were led by the following considerations. For such ions as ^{22}Ne, the DIT occurs in collisions with an orbital angular momentum ℓ close to the

critical one[12-14]. Therefore in the E_ℓ calculations the value of $\ell=\ell_{cr}$ was employed. For the system $^{232}Th+^{22}Ne$, at an ion energy of 172 MeV ℓ_{cr} was calculated from the data on the direct reaction cross section obtained in ref.[5] to be equal to 74 $\hbar$. There are strong arguments for the assumption that the DIT accompany the formation of a double nuclear system (DNS)[12-14]. In the DNS the relative velocity of the nuclei is small and, like a dumbbell, the system rotates as a whole. Since the excitation energy of the DNS reaches 40-60 MeV in our case, one can assume its moment of inertia to be close to the rigid-body one. To calculate E_ℓ we used the formula[15]

$$E = \frac{\hbar^2 \ell_{cr}(\ell_{cr}+1)}{2J} \quad \frac{\mu r_o (A_3^{1/3}+A_4^{1/3})^2}{J},$$

where J is the rigid-body moment of inertia of the DNS,

$$J = \frac{2}{5} M_3 R_3^2 + \frac{2}{5} M_4 R_4^2 + \mu r_o^2 (A_3^{1/3} + A_4^{1/3})^2$$

M_3, M_4 are the masses of the final nuclei, $\mu = \frac{M_3 \cdot M_4}{M_3 + M_4}$, R_3 and R_4 are the mean radii of the matter distribution in the final nuclei[16], and $r_o = 1.46$ fm.

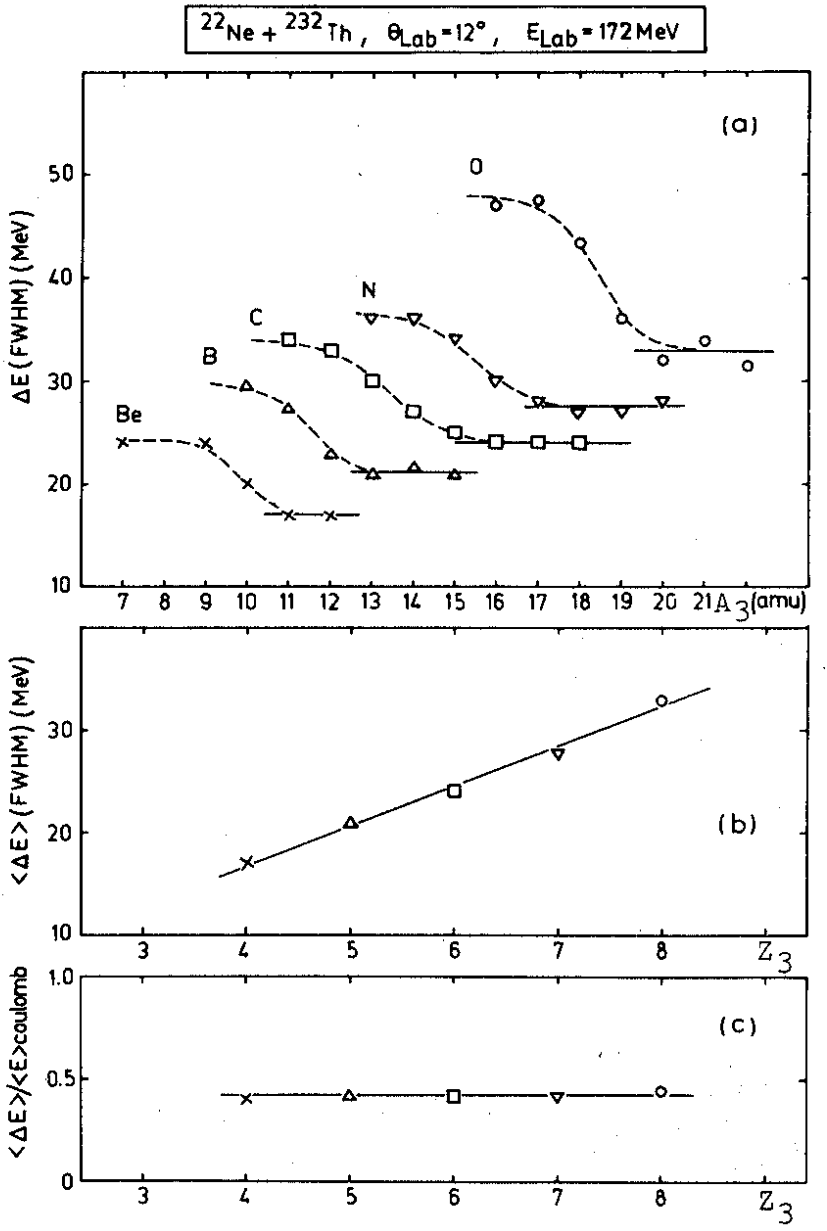
$^{22}Ne + ^{232}Th$, $\theta_{Lab} = 12°$, $E_{Lab} = 172$ MeV
(a)
ΔE (FWHM) (MeV)
O
N
C
B
Be
A_3 (amu)
(b)
<ΔE> (FWHM) (MeV)
Z_3
(c)
<ΔE>/<E>coulomb
Z_3

Fig.4. a)Energy spectra widths ΔE (FWHM) for isotopes with $4 \leq Z \leq 8$ in the CMS as a function of the isotope mass number **A** for an emission angle $\theta_{lab} = 12^{\circ}$. Dashed and solid lines are drawn through experimental points. Solid lines are drawn through the ΔE values for neutron-rich isotopes; b)The widths $\langle \Delta E \rangle$ (FWHM) of the energy spectra for neutron rich isotopes (shown by solid lines in fig.4a) as a function of their atomic numbers Z_3 ; c) The same data normalized to the exit Coulomb barrier for spherical final nuclei with $r_o = 1.46$ fm.

Figure 4a presents the ΔE width (FWHM) of the isotopic energy spectra as a function of mass number **A** . As one can see, a similar behaviour of ΔE(FWHM) is observed for all the elements. The neutron-rich isotopes have a minimum width of the energy spectra which is independent of the mass number of the isotope and remains practically constant for a given element (solid line). With decreasing neutron excess, the ΔE(FWHM) increases sharply and reaches its maximum value in the case of stable and neutron-deficient isotopes.

3.2. Differential Isotopic Production Cross Sections

Table 1 presents the differential cross sections for the production of isotopes, $d\sigma/d\Omega$, obtained by integrating the isotopic energy spectra $d^2\sigma/(d\Omega \cdot dE)$ over energies. The estimated cross sections for the

isotopes whose energy spectra were partially measured are indicated in brackets. Table 1 also shows the values of $Q_{gg} = (M_1 + M_2) - (M_3 + M_4)$ and the Q value in the maximum of the energy spectrum, Q_m. In the calculation of Q_{gg} we used the mass table[17]. One can see that the largest production cross section belongs to isotopes with the least modulo values of Q_{gg}.

Table 1

Differential cross sections $(d\sigma/d\Omega)_{12°}$ in mb/sr for the production of Be, B, C, N, O and F isotopes in the reaction $^{232}Th + ^{22}Ne$ (172 MeV), $Q_{gg} = (M_1 + M_2) - (M_3 + M_4)$, Q_m is the Q value in the maximum of the energy spectrum.

Number of transferred neutrons

Number of transferred protons

	−9	−8	−7	−6	−5	−4	−3	−2	−1	0	+1	+2
−1	A_3, Z_3 $(d\sigma/d\Omega)_{12°}$ (mb/sr) $-Q_{g.g.}$ (MeV) $-Q_m$ (MeV)					^{17}F (0.3) 22.1 (80.0)	^{18}F 4.3 18.9 65.0	^{19}F 14.4 13.3 63.0	^{20}F 11.1 12.8 62.0	^{21}F 8.1 9.9 63.0	^{22}F (3.0) 11.3 (65.0)	^{23}F (0.7) 9.7 (60.0)
−2					^{15}O (0.4) 25.9 (83.0)	^{16}O 21.0 15.2 78.0	^{17}O 17.4 17.0 74.0	^{18}O 16.1 14.3 69.0	^{19}O 5.4 16.9 70.0	^{20}O 3.0 14.4 66.0	^{21}O 0.6 18.6 66.0	^{22}O 0.08 17.0 64.0
−3				^{13}N 0.2 32.0 85.0	^{14}N 4.7 27.6 83.0	^{15}N 17.9 21.9 82.0	^{16}N 4.1 25.7 81.0	^{17}N 3.6 25.1 78.0	^{18}N 0.9 29.2 78.0	^{19}N 0.3 29.9 77.0	^{20}N 0.04 34.8 79.0	^{21}N (0.003) 35.4 (76.0)
−4		^{10}C (0.01) 47.9 (87.0)	^{11}C 0.48 40.9 91.0	^{12}C 13.8 27.3 91.0	^{13}C 13.2 28.5 90.0	^{14}C 11.7 25.7 89.0	^{15}C 2.7 31.1 88.0	^{16}C 1.13 32.3 86.0	^{17}C 0.12 38.6 85.0	^{18}C 0.02 41.0 85.0		
−5			^{10}B 2.4 44.5 95.0	^{11}B 7.2 38.3 98.0	^{12}B 1.4 41.3 99.0	^{13}B 0.64 42.0 98.0	^{14}B 0.036 48.6 98.0	^{15}B 0.013 51.3 98.0				
−6	^{7}Be 0.5 53.8 109.0		^{9}Be 3.5 44.7 109.0	^{10}Be 2.8 43.6 109.0	^{11}Be 0.18 49.9 108.0	^{12}Be 0.05 52.3 106.0						

The isotopic differential cross sections $d\sigma/d\Omega$ as a function of Q_{gg} are presented in fig.5a. Such a systematics was first introduced in our previous work[18]. The generalized Q_{gg}-systematics of the same data is presented in fig.5b. In this case the abscissa axis shows the value of $Q_{gg}-\delta(n)-\delta(p)$, where $\delta(n)$ and $\delta(p)$ are non-pairing corrections for the neutron and proton pairs transferred in the reaction[12-14]. For comparison, the generalized Q_{gg} systematics for the same combination, $^{232}Th+^{22}Ne$, at 172 MeV bombarding energy but at a detection angle of 40° is shown in fig.6. This systematics is based on our previous data[11] with the addition of the newly measured results on differential cross sections for ^{6}He, ^{8}He, ^{19}C and ^{20}C. The comparison of the generalized Q_{gg}-systematics presented in figs.5b and 6 shows that the slope of the element lines and intervals between them practically do not change as one goes from a detection angle of 40° to 12°. It is noteworthy that at an angle of 12° the cross sections for stable and neutron-deficient isotopes fall out of the Q_{gg}-systematics. This deviation is especially considerable in the case of neutron-deficient isotopes. At an angle of 40°, some of the oxygen isotopes fall out of the Q_{gg}-systematics.

The comparison of isotopic differential cross sections $d\sigma/d\theta$ for detection angles of 12° and 40° is given in fig.7. The data are normalized to the cross section at 40°. One can see a considerable difference of the $d\sigma/d\theta$ ratios for isotopes of one and the same element. This difference is the largest for F, O, N and

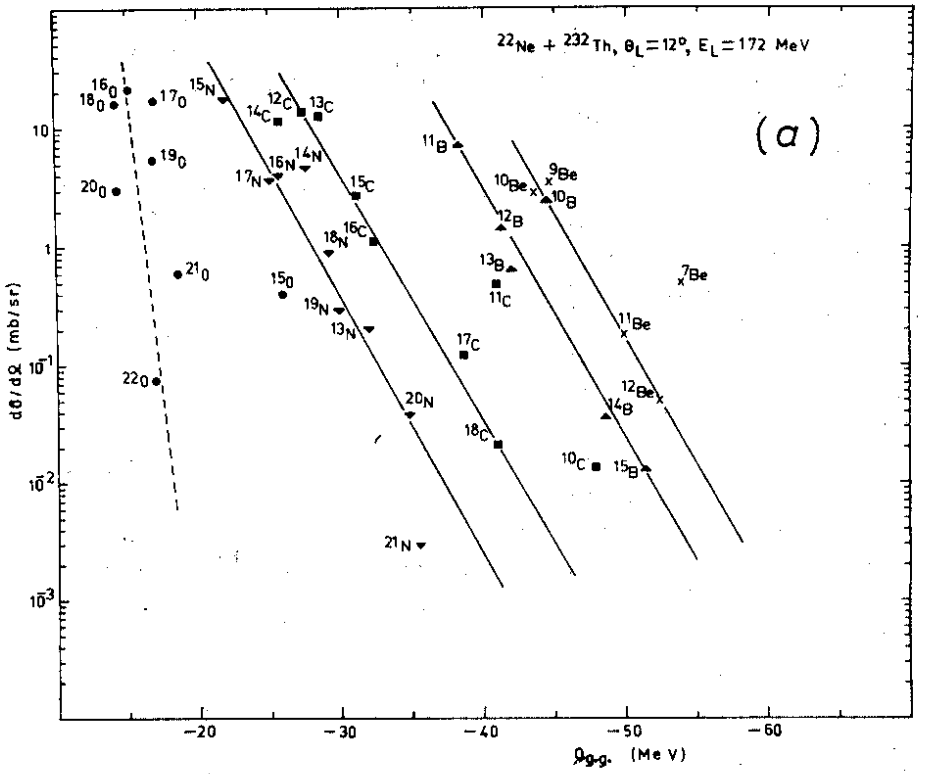

Fig.5a. The Q_{gg}-systematics of differential cross sections $d\sigma/d\Omega$ for transfer reaction products at $\theta_{lab} = 12°$.

C isotopes. Neutron-deficient and stable isotopes of these elements have maximum yields at small angles, while the heaviest isotopes of F, O and N are mainly emitted at an angle close to the grazing one. As the number of transferred nucleons increases (in the case of Be and B isotopes), the difference between the isotopic differential cross sections at 12° and 40° decreases and the angular distribution tends to be isotropic.

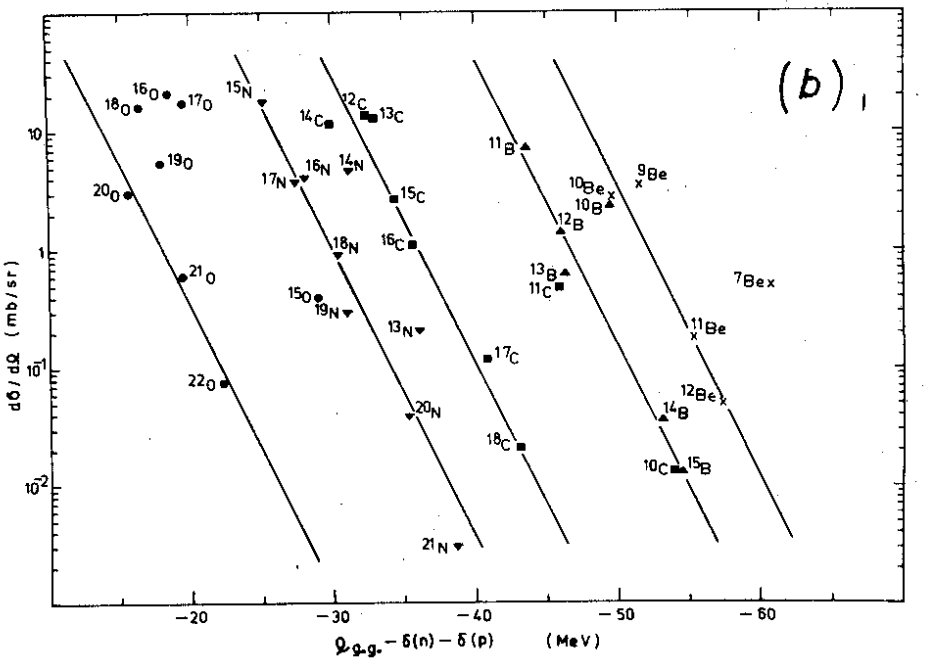

Fig.5b. The generalized Q_{gg}-systematics of differential cross sections $d\sigma/d\Omega$ for transfer reaction products at $\theta_{lab} = 12^{\circ}$.

In the energy spectra and differential cross section measurements at small detection angles one must consider the admixtures of light elements in the target. In the case of thorium these may be oxide or carbonic films. Compound nucleus decay or direct reaction products formed as a result of the interaction of ions with such admixtures can distort noticeably both the shape of the energy spectra and the ratio between the yields of different isotopes. To estimate the possible contribution from such

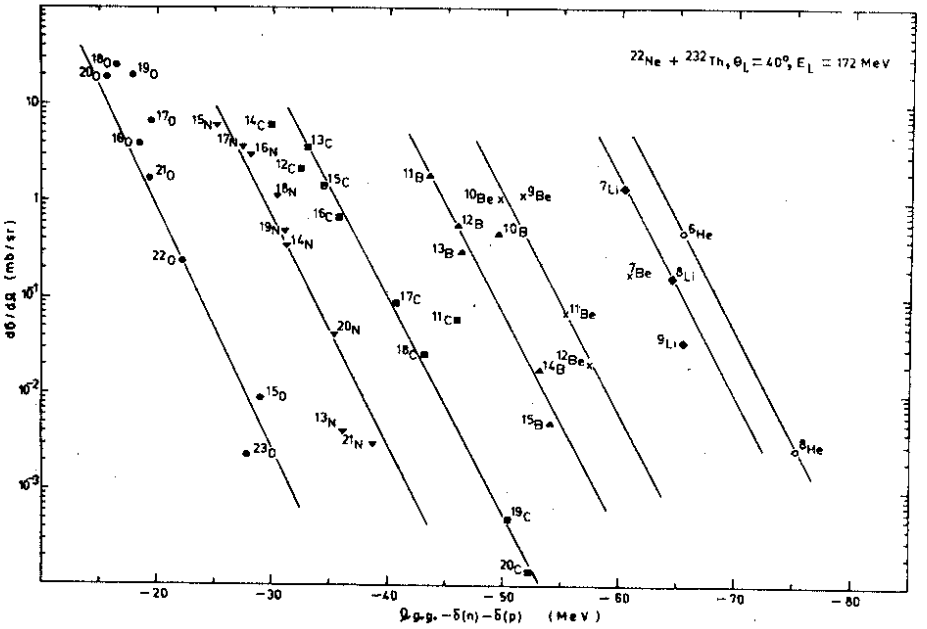

Fig.6. The generalized Q_{gg}-systematics of differential cross sections $d\sigma/d\Omega$ for transfer reaction products at $\theta_{lab} = 40°$.

admixtures, the following control experiment was carried out. A 0.9 mg/cm^2 carbon target was bombarded with 174 MeV ^{22}Ne ions. The energy spectra and isotopic yields for elements with $4 \leq Z \leq 9$ were measured at an angle of 12°. It turned out that the reaction $^{12}C + ^{22}Ne$ produces mainly stable isotopes and those close to the β-stability line. The shape of the energy spectra of these isotopes differs substantially from that of the energy spectra of the same isotopes produced by the reaction $^{232}Th + ^{22}Ne$. On the basis of the data obtained one can conclude

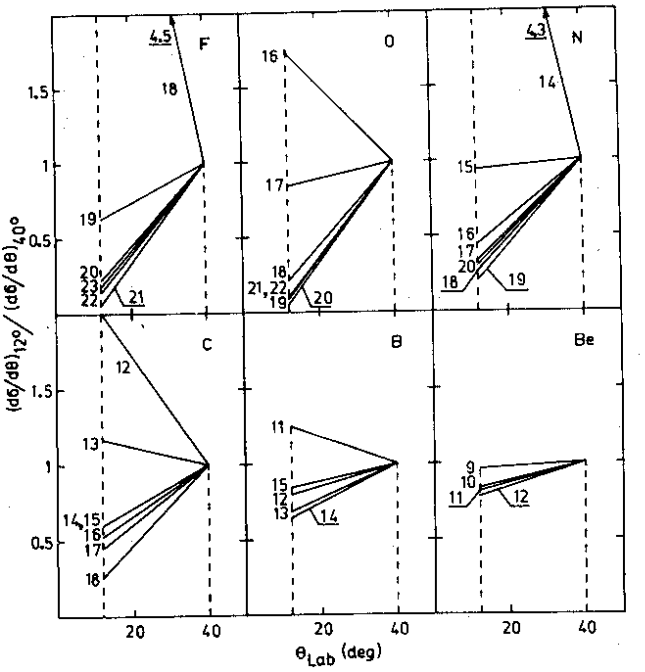

Fig.7. The ratio of isotopic differential cross sections $d\sigma/d\theta$ for emission angles of 12° and 40°. The $d\sigma/d\theta$ value at 40° is taken as a unit of measurement. The isotopic mass numbers are indicated by figures.

that the contribution from light element admixtures in the target are practically negligible.

4. Discussion of Results

On the scale of the entrance angular momenta ℓ, transfer reactions occupy an

interval between the critical angular momentum ℓ_{cr} and the angular momentum of grazing collisions, ℓ_s. Within this interval, the character of the interaction between two nuclei changes substantially as ℓ changes.

In grazing collisions with $\ell \sim \ell_s$, the nuclear surfaces overlap only slightly. Only a small portion of the kinetic energy is transformed to nuclear excitation, and the interaction has the features of a quasi-elastic process. The trajectories of the projectile and transfer reaction products are mainly determined by their scattering in the Coulomb field of the target nucleus. The kinetic energy of the stripping products depends on the number of nucleons left in the nucleus [19]. The interaction time does not exceed a few time 10^{-22} sec.

With a decrease in the entrance angular momentum ℓ the nuclear overlap region increases. A rapidly increasing nuclear attraction deflects the trajectory of light products toward small angles while a growing nuclear friction leads to the dissipation of the collision kinetic energy, which is transformed to nuclear excitation. The orbital angular momentum is partially converted to the spins of the interacting nuclei. The interaction time increases.

In collisions at $\ell \sim \ell_{cr}$ the total dissipation of the kinetic energy occurs. Owing to a high nuclear viscosity the velocity of the relative motion of the nuclei drops practically to zero at the distance of closest approuch between the two nuclei and the double nuclear system (DNS) is formed [12–14]. The decay of the DNS proceeds slowly

on the scale of the characteristic nuclear time ($\sim 1 \times 10^{-22}$ sec) due to the stopping effect of nuclear friction and to the relatively weak repulsive forces involved in collisions at $\ell \sim \ell_{cr}$. During its decay, the DNS, possessing a large angular momentum, may turn by a considerable angle. A substantial number of nucleons may be transferred from one nucleus to the other, and the system itself may become deformed. During the DNS existence, a partial statistical equilibrium may be established in respect of thermal energy and nucleon exchange may occur between the two nuclei. By using this qualitative picture of the interaction between two complex nuclei as a starting point we shall make an attempt to interpret the data obtained and reveal some specific features of the formation of different isotopes.

One can see from fig.3a that the energy maxima E_{max} in the energy spectra of stable and neutron-rich isotopes increase with A . In the framework of the liquid drop model the decay of the intermediate nuclear system without its deformation should have given the A dependence of E_{max} shown by the solid line $E_c + E\ell$. The system deformation would have led to a decrease in the sum of the exit Coulomb and centrifugal barriers, $E_c + E_\ell$. In this case the solid lines would be displaced downward in the direction of smaller energies. The experimentally obtained E_{max} versus A dependence indicates that the final nuclei have a noticeable relative velocity prior to scission.

The E_{max} values for the data obtained at 12° and 40° are compared in fig.3b. One

can see that E_{max} for the isotopes of all the elements detected at an angle of 12° are close to the potential barrier, $E_c + E_\ell$. The same is valid for the multinucleon transfer reaction products, Be and B, detected at 40°. The fact that the energies E_{max} in the energy spectrum maxima are close to the sum of the exit Coulomb and centrifugal barriers, $E_c + E_\ell$, implies practically the full dissipation of the kinetic energy during the interaction of two nuclei. At an angle of 40°, the kinetic energy of the products increases well over $(E_c + E_\ell)$ with a decrease in the number of protons transferred. This indicates that quasi-elastic and inelastic processes are the main contributors to the isotopic production cross section.

Figures 4 and 7 show that the ΔE(FWHM) widths and the relative yields at 12° and 40° are different for two groups of isotopes, the first comprising stable and neutron-deficient isotopes, and the second comprising some neutron-rich isotopes. In the first group, ΔE(FWHM) is substantially large; these isotopes are emitted mainly at small angles, their production cross sections at an angle of 12° fall outside the Q_{gg}-systematics. From our point of view, this difference is due to a contribution to the yield of isotopes in the first group from secondary processes such as α-particle and neutron evaporation from the excited ^{22}Ne and transfer reaction products /20/. In the bombardment of ^{232}Th with 172 MeV ^{22}Ne ions, an energy of about (40-60) MeV can be converted to nuclear excitation. A noticeable part of this energy may remain in the inelastically scattered ^{22}Ne nucleus or a light transfer reaction product.

Since the ^{22}Ne projectile is characterized by neutron excess, and the binding energy of α-particles in light nuclei is low, neutrons and α-particles are mainly emitted from excited light products. As a result, stable and neutron-deficient isotopes are formed as secondary products. The yield of stable isotopes increases and their production cross section turns out to be larger than that expected from the Q_{gg}-systematics based on production cross sections for neutron-rich isotopes. Useful relevant information can be provided by α-particles, which seem to form as a result of evaporation from excited light products. In our preliminary experiments involving the bombardment of ^{232}Th with 172 MeV ^{22}Ne ions as well as in other work /21/, a considerable number of α-particles were observed with a strong forward peaking in their angular distribution.

The increase in the width of the energy spectra, ΔE (FWHM), expected due to the superposition of two different nuclear processes, the nucleon transfer and sequential decay, is observed experimentally (see fig.4a).

It is especially interesting to analyze the mechanism of transfer reactions by studying the behaviour of the ΔE (FWHM) spectra of the neutron-rich isotopes for which the contribution from secondary processes is negligible. It should first be noted that the energy spectra of transfer reaction products extend over several tens of MeV below the exit Coulomb barriers. It is hardly possible to interpret the appearance of low energy particles as being due to

the potential barrier penetration. First, the barrier penetration for such heavy particles decreases with energy more sharply, and, second, there is no pocket at all in the nuclear interaction potential in the exit channel at $\ell > \ell_{cr}$. One can assume that the shape of the energy spectrum in deep inelastic transfers, in the vicinity of the maximum at least, is determined by statistical fluctuations of distance **R** between the centres of the final nuclei at scission. If these **R** fluctuations depend weakly on the light fragment and are mainly determined by the heavy nucleus, then $\langle \Delta E \rangle$ will be proportinal to $(Z_3 \times Z_4)$ or Z_3 of the light fragment since Z_4 of the heavy fragment changes inconsiderably in the course of the transfer of several protons. The experimental values of $\langle \Delta E \rangle$ averaged over the spectra widths for the neutron-rich isotopes shown in fig.4a by a solid line are presented in fig.4b. One can see the linear dependence of $\langle \Delta E \rangle$ on the light product atomic number. If one calculates the average Coulomb barrier $\langle E_c \rangle$ for the same neutron-rich isotopes and normalize $\langle \Delta E \rangle$ to $\langle E_c \rangle$, the straight line shown in fig.4c is obtained.

Now we shall turn to the Q_{gg}-systematics. It was noted in ref.[22] that the Q_{gg} dependence cannot be interpreted in the framework of classical direct processes. To interpret it, the authors of ref.[22] introduced the concept of partial statistical equilibrium. In refs.[12-14] the hypothesis about the formation of a long-lived double nuclear system (the DNS) with a lifetime of 1-2 x 10^{-21} sec was employed as an argument for the possible

partial statistical equilibrium. The authors of refs.[12-14] introduced the generalized Q_{gg} -systematics which took into account the nonpairing of the nucleon pairs transferred from the donor-nucleus to the acceptor one. For $d\sigma/d\Omega$ the following expression has been obtained

$$d\sigma/d\Omega \sim \exp[(Q_{gg} + \Delta E_c + \Delta E_{rot} - \delta(n) - \delta(p))/T]$$

where ΔE_c is a variation of the DNS Coulomb energy due to the proton transfer; ΔE_{rot} is a variation of the DNS rotational energy with a change in the system moment of inertia due to the nucleon transfer; and $\delta(n)$ and $\delta(p)$ are non-pairing corrections for neutron and proton pairs transfers, respectively. In terms of this concept the slope of the element lines characterizes the "temperature" of partial statistical equilibrium. It is interesting to compare the T values corresponding to angles of 12° and 40°. They coincide within experimental accuracy, i.e., $T(12^\circ)=1.8$ MeV and $T(40^\circ)=1.9$ MeV.

If we consider the data obtained from the point of view of producing extremely neutron-rich isotopes of light elements, the following can be noted. In producing isotopes close in Z to the initial nucleus (F, O and N) it is advantageous to place the detecting system at an angle close to the grazing one. For the B and Be isotopes produced by multinucleon transfer reactions, the maximum yields correspond to small angles. However, at small angles the intensity of the elastically and inelastically

scattered ions increases sharply. Therefore in this case the grazing angle can also turn out more suitable.

5. Conclusions

In the bombardment of ^{232}Th with ^{22}Ne ions at an energy of 172 MeV, all of the light fragments with $4 \leq Z \leq 9$ detected at an emission angle of 12° are the products of deep inelastic reactions. Among these products, very neutron-rich isotopes seem to be formed directly in transfer reactions without emission of secondary particles. Their production cross section obeys the Q_{gg} -systematics. The secondary processes, the α-particle and neutron emission from the excited ^{22}Ne and light transfer reaction products, contribute substantially to the production cross sections for stable and neutron-deficient isotopes. This leads to the widening of the energy spectra for these isotopes and to an increase in their yields. The yield of neutron-deficient isotopes is mainly determined by secondary processes.

The slope of the element lines in the generalized Q_{gg}-systematics does not change as one goes from an emission angle of 12° to 40°.

The energy versus A variations in the maxima of isotopic yields indicate a noticeable relative velocity of the nuclei at the moment of scission. This can be regarded as an evidence for the conservation, to a certain extent, of the individualities of the interacting nuclei in deep inelastic collisions.

In producing the isotopes of light elements with an extreme neutron excess by transfer reactions induced by heavy ions it is preferable to use detection angles close to the grazing angle.

The authors express their deep appreciation to Professor G.N.Flerov for his stimulating interest to the work. Thanks are also due to the staff of the U-300 cyclotron for providing an intense ^{22}Ne ion beam, the radioelectronic department of the Laboratory of Nuclear Reactions for the stable operation of the electronic apparatus, and A.N.Mezentsev for his help in calculating the pairing corrections.

Reference

1. J.Wilczynski, V.V.Volkov, P.Decowski. Yad.Fiz., 5, 942 (1967).
2. G.F.Gridnev, V.V.Volkov, J.Wilczynski. Nucl.Phys., A142, 385 (1970).
3. J.Galin, D.Guerreau, M.Lefort, J.Peter, X.Tarrago, R.Basile. Nucl.Phys., A159, 461 (1970).
4. A.G.Artukh, G.F.Gridnev, V.L.Mikheev, V.V.Volkov, J.Wilczynski. Nucl.Phys., A215, 91 (1973).
5. A.G.Artukh, J.Wilczynski, V.V.Volkov, G.F.Gridnev, V.L.Mikheev. Yad.Fiz., 17, 1126 (1973).
6. F.Hanappe, M.Lefort, C.Ngo, J.Peter, B.Tamain. Phys.Rev.Lett., 32, 738 (1974).
7. L.G.Moretto, D.Hannemann, R.C.Jared, R.C.Gatti, S.G.Thompson. Third Symp. on Phys. and Chemistry of Fission. Rochester,1973,USA; LBL-1966, July 1973.

8. K.L.Wolf, J.P.Unik, J.R.Huizenga, J.Birkelund, H.Freisleben, V.E.Viola. Phys.Rev.Lett., 33, 1105 (1974).
9. A.G.Artukh, V.V.Avdeichikov, J.Ero, G.F.Gridnev, V.L.Mikheev, V.V.Volkov. Nucl.Instr. and Meth., 83, 72 (1970).
10. M.Lefort, Y.Le Beyec, J.Peter. Report IPNO-RC-73-04 (1973); Yu.Ts.Oganessian, Yu.E.Penionzhkevich, K.A.Gavrilov, Kim De En. Preprint JINR P7-7863, Dubna, 1974.
11. A.G.Artukh, G.F.Gridnev, V.L.Mikheev, V.V.Volkov, J.Wilczynski. Nucl.Phys., A211, 299 (1973).
12. A.G.Artukh, V.V.Volkov, G.F.Gridnev, V.L.Mikheev. Izvestija AN USSR, seria fiz., 39, 2 (1975).
13. V.V.Volkov. Proc.Int.Conf. on Reactions between Complex Nuclei, Nashville, 1974, ed. by R.L.Robinson e.a., vol. 2, Invited Paper (North Holland Publ. Co., 1974), p. 363.
14. V.V.Volkov. Int. Symp. on Classical and Quantum Mech. Aspects of H.I.Collisions, Heidelberg, 1974, ed. Springer-Verlag, Berlin.
15. R.Bass. Nucl. Phys., A231, 45 (1974).
16. L.R.B.Elton. Nuclear Sizes, (Oxford University Press, London, 1961).
17. G.T.Garvey, W.J.Gerace, R.L.Jaffe, I.Talmi ,and I.Kelson. Rev.Mod.Phys., 41, 51 (1969).
18. A.G.Artukh, V.V.Avdeichikov, J.Ero, G.F.Gridnev, V.L.Mikheev, V.V.Volkov, J.Wilczynski. Nucl.Phys., A160, 511 (1971).
19. P.J.Siemens, J.P.Bondorf, D.H.E.Gross, F.Dickmann. Phys. Lett.,36B, 24 (1971).

20. J.P.Bondorf, W.Norenberg. Phys.Lett., 44B, 487 (1973).
21. H.C.Britt, A.R.Quinton. Phys.Rev., 124, 877 (1961); A.Kapustsyk, V.P.Perelygin, S.P.Tretyakova, L.V.Ukraintseva. Yad.Fiz., 6, 1142 (1966).
22. J.P.Bondorf, F.Dickmann, D.H.E.Gross, P.J.Siemens. J. de Phys., 32, C6-145 (1971).

Received by Publishing Department
on August 16, 1976.